

# Synthesis of Fluoridated Polymer for Self-Assembly Nanovaccines with Antigen and Oligodeoxynucleotides for Cancer Immunotherapy

Isabella Xingyi Li

Portsmouth Abbey School, USA

## ABSTRACT

Cancer immunotherapy represents a type of cancer treatment that represses the disease by triggering immune responses. Cancer vaccines play a crucial role in this approach by delivering tumor-specific antigens into antigen-presenting cells which causes an antigen-specific immune response to eliminate cancer cells by effective delivery of antigens into antigen-presenting cells. Effective antigen presentation is critical in eliciting antigen-specific immune responses. Polymers such as dendrimers and polyethyleneimines (PEIs) have been reported for their potential application in delivering antigens and have functioned as vaccine vehicles. However, the cytotoxicity of PEI limits its application as a safe antigen-delivering vector. The fluorination effect can be utilized to reduce cytotoxicity and enhance the efficiency of antigen delivery by forming fluorinated PEI (F-PEI), which can be produced by fluorinating PEI with fluoroalkanes. Due to the low lipophobicity of modified fluoroalkyl chains on polymers, F-PEIs-based nanovaccine for delivering the model antigen ovalbumin (OVA) along with a vaccine adjuvant can induce antigen-specific immune responses targeting cancer. The F-PEI is capable of loading OVA and CpG oligonucleotides (CpG ODN) through electrostatic attraction. The resulting nanovaccine — F-PEI/OVA/CpG — exerts negligible effects on cell viability and effectively enters antigen-presenting cells. According to the observation, F-PEI/OVA/CpG activates bone marrow dendritic cells (BMDCs)' maturation by upregulating the expression of CD80 protein and CD86 protein, which serve as mature markers for BMDCs. Future research related to F-PEI/OVA/CpG could be extended to different antigens (e.g., neoantigens) and potential clinical applications.

## Introduction

Cancer immunotherapy is a type of cancer treatment that works by increasing the efficiency of the immune system (Zhang et al., 2020). Tracing back to the 19th century, William Bradley Coley attempted to apply Coley's toxin in the treatment of cancer patients (Wiemann & Starnes, 1994). However, due to the risk of infection leading to fatalities, the recovery and effect remains controversial. Despite the unideal outcomes of early immunotherapies for cancer, current studies have demonstrated the effectiveness of treating cancer by inducing immune system responses, such as adoptive cell transfer (ACT) (Rosenberg, 2011), immune checkpoint inhibitors (ICIs) (Shiravand et al., 2022), and anti-cancer vaccine treatments (Vermaelen, 2019). One notable example is immune checkpoint inhibitors like the anti-PD-1 antibody nivolumab, designed to selectively bind to PD-1 on T cells, thereby relieving inhibitions imposed by cancer cells (Ribas & Wolchok, 2018).

Introducing tumor-specific antigens into antigen-presenting cells, cancer vaccine eliminate cancer cells by triggering a targeted immune response. This approach has demonstrated notable success, particularly evident in the human papillomavirus infection (HPV) vaccination (Lehtinen & Dillner, 2013). Moreover, adjuvants play a crucial role in augmenting the efficacy of cancer vaccines by stimulating antigen-presenting cells, thereby boosting the immune response (Shrestha, 2014). For instance, CpG oligonucleotides (ODN) function

as vaccine adjuvants by activating Toll-like receptor 9 (TLR9) found on professional antigen-presenting cells. This activation stimulates innate immunity to generate various cytokines beneficial for CD8+ T cell-mediated anti-cancer immunity (Bode et al., 2011; Krieg, 2006). Effective delivery of antigens to antigen-presenting cells remains a challenge. Various materials, such as lipid-based vehicles, polymers, inorganic-based vehicles, and bio-inspired vehicles, have been explored as potential antigen delivery vehicle (Vivero-Escoto et al., 2010; ;). Although lipid-based nanoparticles have received FDA approval for delivering diverse therapeutic agents and antigens, cellular toxicity and high cost is a concern that hinders their application (Shrestha et al., 2014; Neubi et al., 2018; Liechty et al. 2010).

In recent developments, fluorinated dendrimers and polyethyleneimines (PEIs) have emerged as antigen delivery systems (Zhang et al., 2018). These modified cationic polymers, containing fluorinated PEIs, possess a notable feature due to their reduced lipophobicity as a result of the introduced fluoroalkyl chains (Cametti et al., 2012). This characteristic enables the efficient delivery of antigens into dendritic cells (DCs) by major histocompatibility complex class I (MHC-I)-mediated antigen presentation — a crucial element in cellular immunity. Despite the impressive antigen delivery capability of fluorinated PEIs, challenges exist regarding their ability to evoke immunity in complex conditions and concerns about the potential impact on human body.

This study aims to investigate the self-assembly of fluorinated PEI (F-PEI) into nanoparticles with negatively charged model antigens such as ovalbumin (OVA) and CpG ODN, as illustrated in Figure 1. This approach is anticipated to improve antigen delivery while simultaneously bolstering innate immunity by activating the TLR9 pathway, thus contributing to cellular immunity. The significance of this study lies in its innovative methods for developing cancer vaccines using fluorinated PEI known for its ease of preparation. Furthermore, the application of fluorinated PEI as a delivery system for therapeutic gene agents, such as mRNA, is also under consideration. This project may yield a standardized method for preparing nanovaccines based on fluorinated polymers and provide insights into the extent to which vaccine efficiency can be enhanced through fluorination. Preliminary findings indicate the low cellular toxicity of fluorinated PEI suggests the possibility of extending into animal experiments and clinical trials.

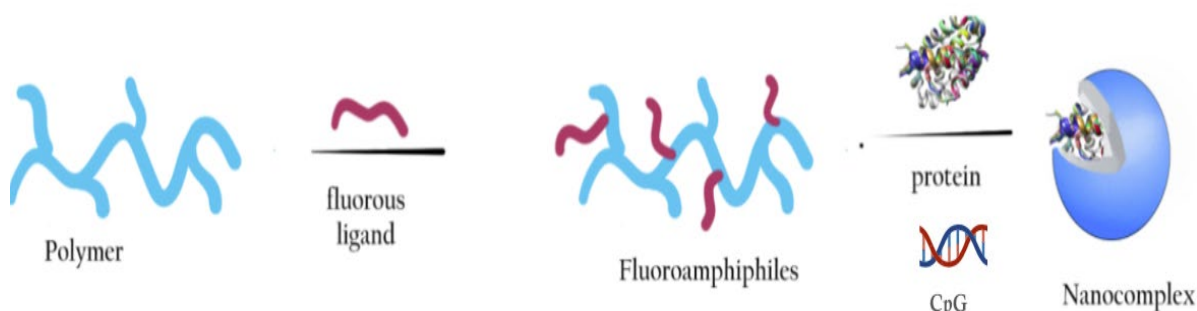


**Figure 1.** Scheme

## Materials and Methods

### Cell Culture

Cultivate RAW264.7 cells in DMEM supplemented with 10% Fetal Bovine Serum (FBS) and 1% Penicillin Streptomycin (Pen/Strep). DC2.4 cells were cultured in RPMI supplemented with 10% FBS and 1% Pen/Strep.

The methods of cell culture and passage were described as following. Prepare culture vessels, including new Petri dishes and centrifuge tubes. Introduce the requisite culture media to facilitate cellular growth. Allow

the cells to proliferate until reaching a density within the range of 80%-90%. Subsequently, harvest the cells and subject them to 1-2 washes with cell culture medium to eliminate extraneous debris and waste materials. Initiate cell detachment by employing trypsin enzyme at 37°C, utilizing agitation to expedite the process. Arrest enzymatic activity by introducing culture medium containing 10% fetal bovine serum. Homogenously distribute the resultant supernatant into the centrifuge tube, followed by centrifugation to remove supernatant and cellular debris. Reconstitute the cells in the suspension with a judicious quantity of culture medium. Transfer the prepared cell suspension into a fresh culture dish, ensuring uniform distribution. Position the culture dish in an environment conducive to cellular growth, exercising control over parameters such as temperature, humidity, and CO<sub>2</sub> concentration.

### Preparation of F-PEI/OVA/CpG

As shown in Figure 2, the branched PEIs is fluorinated by dropwise addition of epoxides bearing fluoroalkanes into PEI in methanol at a molar ratios of 36:1. After stirring for 48 h at RT, the fluorinated PEI (F-PEI) is purified from raw products with MWCO 3000 Da dialysis bag against methanol and ddH<sub>2</sub>O. Then the obtained F-PEI is mixed with OVA at a weight ration of 0.5:1 of 1:1 in ddH<sub>2</sub>O and 10 µg/mL CpG ODN for 25 min to form F-PEI/OVA/CpG nanoparticle, which would be characterized by transmission electron microscopy (TEM) and dynamic light scattering (DLS).

### FITC-Conjugated OVA

Reconstitute OVA stock to 10 mg/mL concentration with ddH<sub>2</sub>O. The NHS-Fluorescein is dissolved in DMSO at a concentration of 10 mg/mL. The NHS-Fluorescein is mixed with OVA at a molar ratio of 20:1 and stirred 2 h on ice. Then the products is purified with gel filtration to remove non-conjugated NHS-fluorescein.

### Cytotoxicity Test

Raw264.7 and DC2.4 will be used as target cells to test the cytotoxicity of F-PEI/OVA. Briefly, incubate cells in 96-well plate for 24 h to adherent, add 0, 10, 20, 50, 100, 200, and 300 µg/mL of F-PEI/OVA/CpG or F-PEI/OVA per well, respectively. After 24 h, add 10 µL of CCK-8 solution to each well and culture in cell incubator for 2 h. Absorbance was measured at 450 nm wavelength with microplate reader to calculate cytotoxicity.

### Flow Cytometer

For cellular uptake, DC2.4 and RAW264.7 are co-cultured with 10 µg/mL OVA-FITC, 10 µg/mL F-PEI/OVA-FITC, 10 µg/mL F-PEI/OVA-FITC/CpG for 8 h in CO<sub>2</sub> incubator. Then cells were collected and centrifuge at 1200 rpm for 3 min. After 3-times washes, cells are resuspended with PBS complemented with 1% FBS then detected FITC fluorescence signals with flow cytometer CytoFLEX S (Beckman). For DC maturation, differently treated BMDCs are centrifuged to collect and stained with anti-CD11c-FITC, anti-CD86-PE, anti-CD80-APC for 1h at room temperature. After 3-times washes, cells are detected fluorescence signals with flow cytometer.

## Laser Scanning Confocal Microscopy

Briefly, DC2.4 and RAW264.7 are co-cultured with 10  $\mu\text{g/mL}$  OVA-FITC, 10  $\mu\text{g/mL}$  F-PEI/OVA-FITC, 10  $\mu\text{g/mL}$  F-PEI/OVA-FITC/CpG in 3.5 cm dishes for 8 h in CO<sub>2</sub> incubator. After 3-times washes, cells are stained with Hoechst dye for 30 min, which could bind to DNA in nucleus and display fluorescence to facilitate recognizing location of cells. After 3-times washes, added 1 mL DMEM or RPMI culture medium into 3.5 cm dishes, then imaging with IX73 (Olympus) laser scanning confocal microscopy.

## BMDCs Maturation

BMDCs were collected and inoculated in 24-well plate at  $5 \times 10^5/\text{mL}$ , 1 mL/well. BMDCs are co-cultured with 10  $\mu\text{g/mL}$  OVA, 10  $\mu\text{g/mL}$  F-PEI/OVA, 10  $\mu\text{g/mL}$  F-PEI/OVA/CpG for 24 h in CO<sub>2</sub> incubator. Then cells are centrifuged to collect and stained with anti-CD11c-FITC, anti-CD86-PE, anti-CD80-APC for 1 h at room temperature. After 3-times washes, cells are detected fluorescence signals with flow cytometer.

## Results and Discussion

### Synthesis and Characterization of F-PEI/OVA/CpG Nanovaccine

The preparation method was described in the section of Materials and Methods in this paper. And the protocol was illustrated in Figure 2.

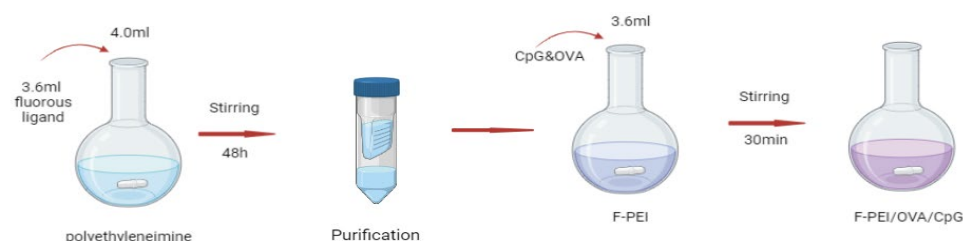


**Figure 2.** Protocol. The prepared F-PEI/OVA/CpG has a average diameter of 200 nm, and the DLS data displayed that the hydrodynamic size of F-PEI/OVA/CpG is  $256.7 \pm 2.1$

According to the same protocol, different nanoparticles were prepared as control groups, such as PEI/OVA, PEI/OVA/CpG, F-PEI/OVA. Then different nanovaccine were characterized with dynamic light scattering (DLS). F-PEI/OVA/CpG was tested with transmission electron microscopy (TEM). As shown in Figure 3a, (Figure 3d). Meanwhile, the zeta potential of F-PEI/OVA/CpG was determined by DLS as  $36.8 \pm 4.5$  and the PDI was 0.31 (Figure 3b and Figure 3d), which indicate that the prepared F-PEI/OVA/CpG has good dispersity. Next, we wonder if different CpG ratio could influence the surface charge, so we use CpG masses as variables in preparing F-PEI/OVA/CpG, the obtained nanoparticle posses similar diameter and zeta potential (Figure 3c).

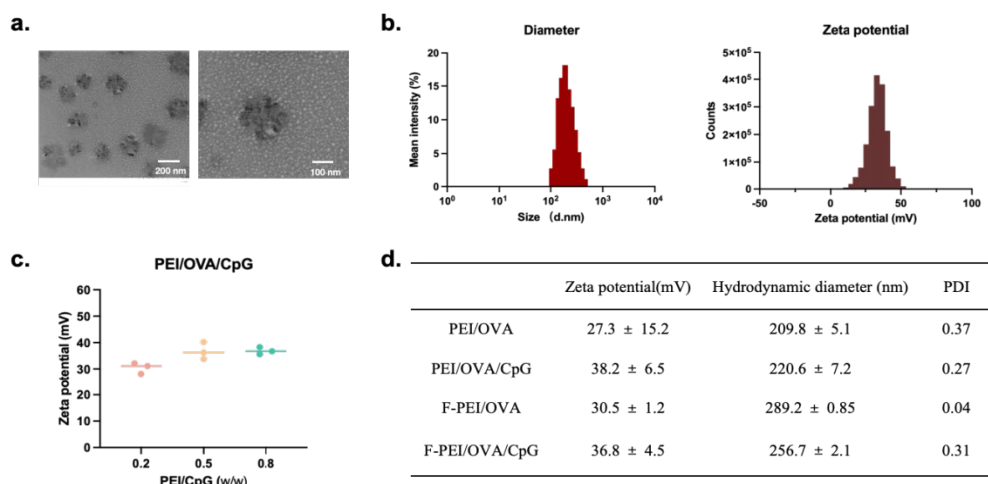


**Figure 3.** Characterization

### PEI/OVA/CpG Cytotoxicity to RAW264.7 and DC2.4 Cells

Before the obtained nanovaccine F-PEI/OVA/CpG was used in cells, we have tested the cytotoxicity of F-PEI/OVA/CpG towards two different celllines of antigen-presenting cells—DC2.4 and RAW264.7. Briefly, Raw264.7 and DC2.4 were incubated with F-PEI/OVA/CpG or F-PEI/OVA at different concentration in 96-well plate. Then use CCK-8 solution to each well to boost color reaction and absorbance of each well was measured at 450 nm wavelength with microplate reader to calculate cytotoxicity.

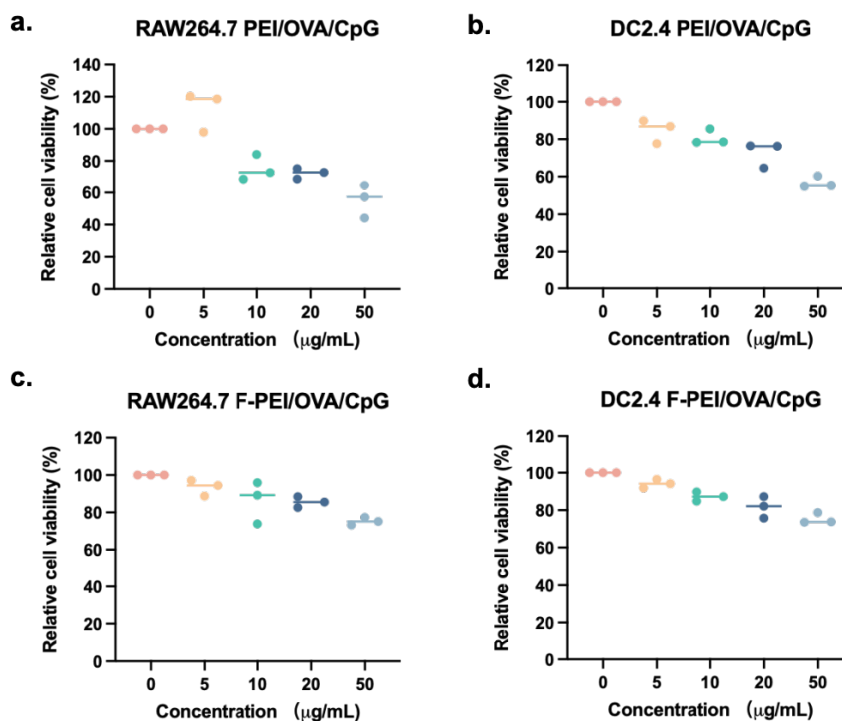


**Figure 4.** Cytotoxicity

As shown in Figure 4a, PEI/OVA/CpG nanoparticle reduced the viability of RAW264.7 cells to mere about 50% after 24 h coculture at concentration of 50  $\mu\text{g/mL}$ , the similar results was observed in PEI/OVA/CpG treated DC2.4 group (Figure 4b). These data indicates that PEI as vaccine vector shows relatively severe cytotoxicity toward antigen-presenting cell. However, after modified with fluoruous ligand, F-PEI/OVA/CpG slightly reduced cell viability to about 80% even at a high material concetration of 50  $\mu\text{g/mL}$  (Figure 4c). The same experimental appearance was observed in F-PEI/OVA/CpG treated DC2.4 group (Figure 4d). All together, these results indicate that F-PEI/OVA/CpG posses good biocompatibility compared to PEI/OVA/CpG.

### The Cellular Uptake Efficiency of PEI/OVA/CpG

We conducted experiments to assess the effectiveness of F-PEI/OVA/CpG in entering antigen-presenting cells. In short, FITC-labeled OVA and CpG was mixed with F-PEI to create fluorescence-labeled nanoparticles, and the resulting F-PEI/OVA-FITC/CpG was co-cultured with RAW264.7 or DC2.4 cells for 4 hours. Following co-culture, the FITC signal in cells was detected using FACS, and Flowjo was used for data analysis. As show in Figure 5a, the scatter diagram of cells treated with OVA-FITC displayed about 5% positive cells, which means the efficiency of OVA-FITC entering cells is low. Also, the histogram illustrates that the peak of cells treated with OVA-FITC alone exhibits a slight shift compared to untreated cells (Figure 5b). However, cells treated with F-PEI/OVA-FITC display a significant shift in the peak compared to those treated with PEI/OVA-FITC, indicating that the modification of fluoruous on PEI effectively enhances the cellular uptake of the antigen. Similar results were observed in the DC2.4 group (Figure 5c). These findings indicate that AuNP-PEI efficiently delivers the antigen into antigen-presenting cells.

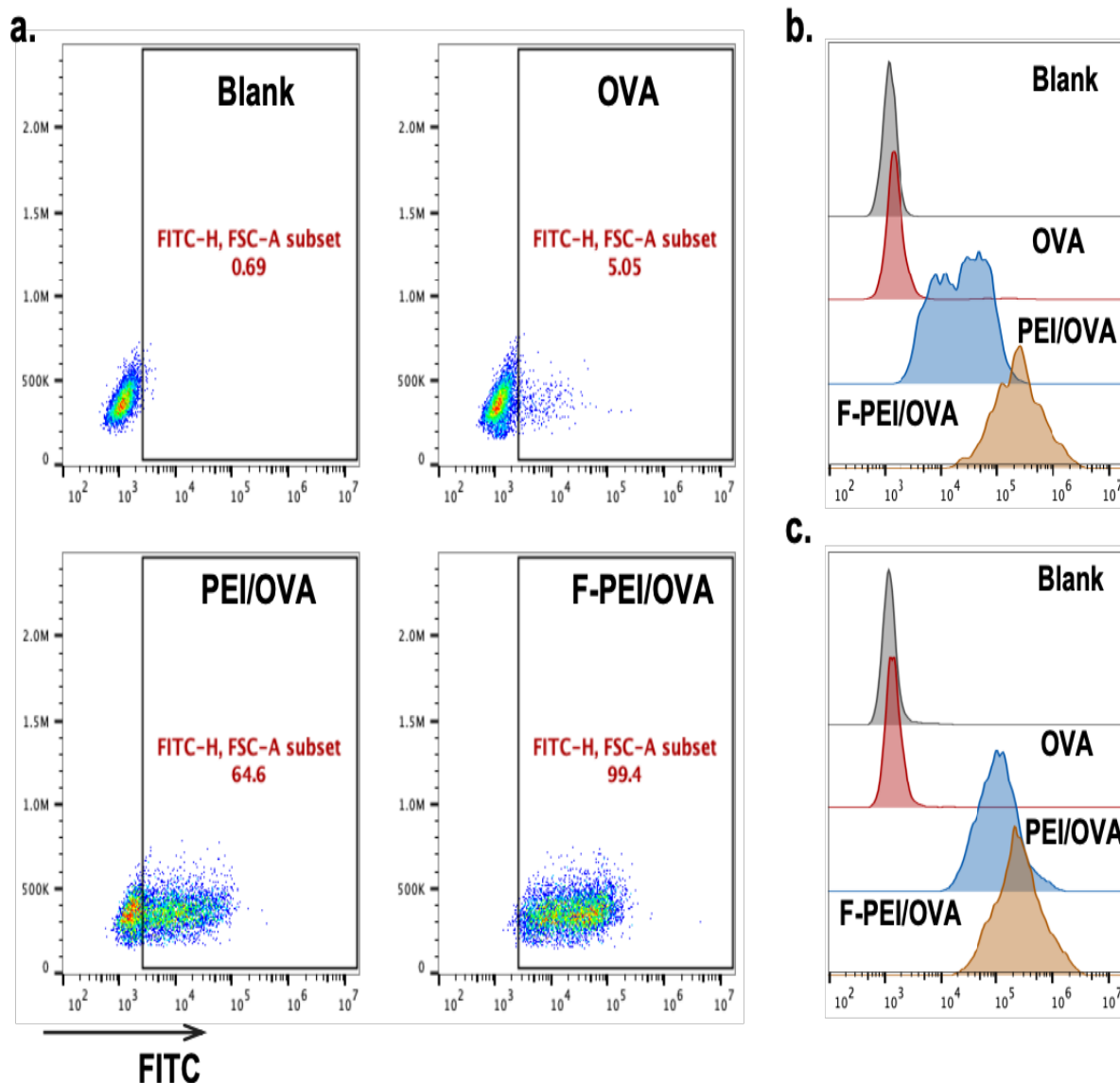


**Figure 5.** The cellular uptake efficiency of PEI/OVA/CpG determined by FACS.

To further assess the internalization of F-PEI/OVA by antigen-presenting cells, we utilized confocal fluorescence microscopy. Initially, we co-cultured F-PEI/OVA-FITC with RAW264.7 and DC2.4 cells. Following the culture, the cells underwent PBS washing. Subsequently, confocal fluorescence microscopy was employed to evaluate the extent of cellular uptake, as depicted in the provided charts. The OVA protein was visualized as a green glow emitted by FITC, while the cells in the dark field were represented by a blue glow generated by Hoechst, which binds with DNA in the nucleus of cells (Figure 6). By merging the two channels, we could ascertain whether the fluorescence-conjugated OVA had penetrated the cells (Figure 6). The charts illustrate that F-PEI/OVA-FITC and PEI/OVA-FITC effectively delivered antigens, accompanied by fluorescence within the cells (Figure 6). In summary, the findings from FACS and fluorescence imaging collectively suggest the efficient cellular uptake of F-PEI/OVA/CpG.



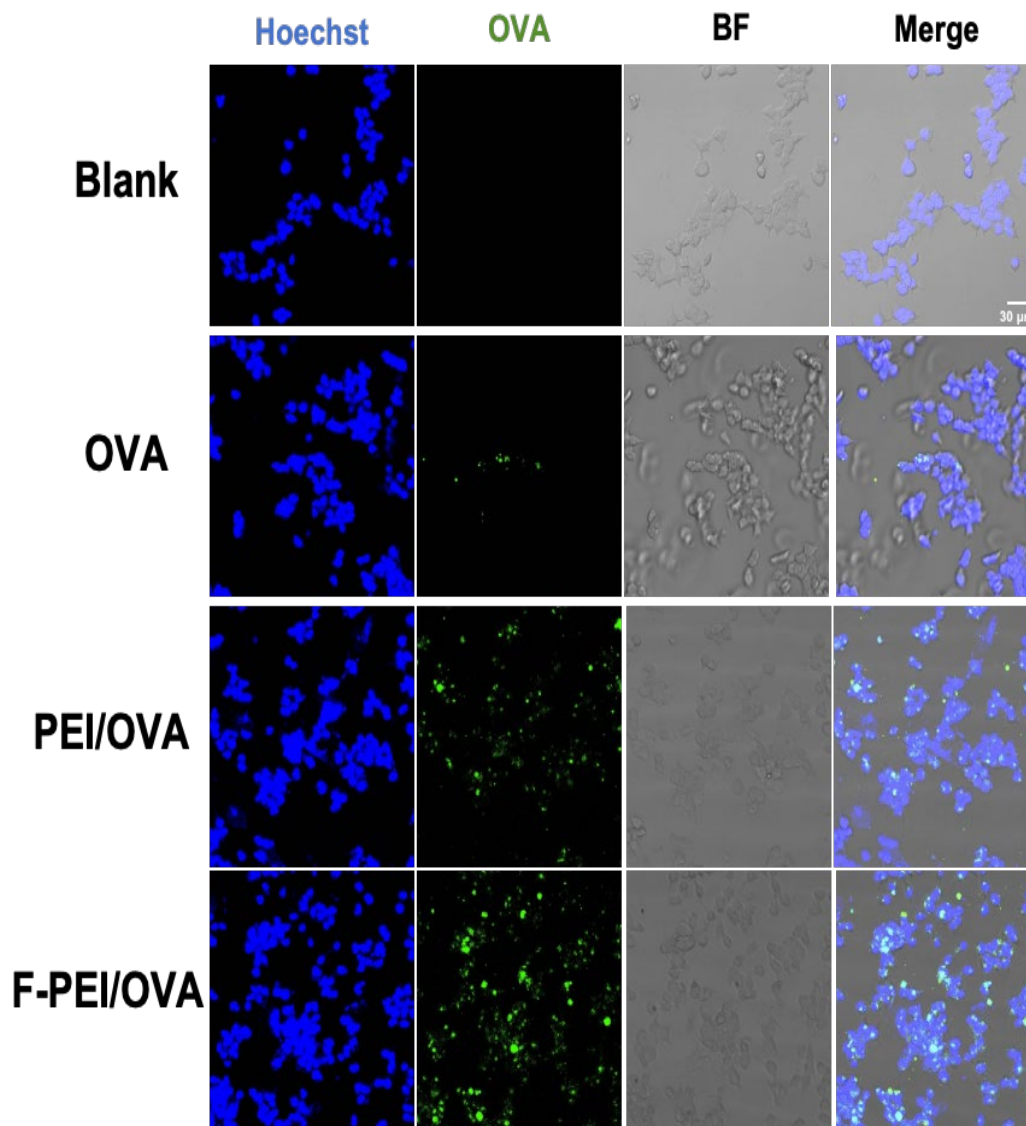


**Figure 6.** The cellular uptake efficiency of PEI/OVA/CpG determined by Laser Scanning Confocal Microscopy.

### PEI/OVA/CpG Stimulate BMDCs to Mature

By employing flow cytometry, we assessed the impact of F-PEI/OVA and PEI/OVA on the maturation of DC cells. The x-axis corresponds to CD86 maturation, while the y-axis represents CD80 maturation, which both are the marker of mature DCs. F-PEI/OVA was co-cultured with BMDCs for 24 hours. Subsequently, the cells were labeled with fluorescence antibodies for 1 h at room temperature, and their CD86 and CD80 expressions were analyzed. Figure 7a presents the scatter diagram of untreated cells, cells treated with LPS, cells treated with OVA only, cells treated with PEI/OVA/CpG, and cells treated with F-PEI/OVA/CpG, showcasing maturation results of 1.79%, 66.5%, 11.4%, 29.9%, and 49.3%, respectively (Figure 7a). And the statistic results of three times experiments also display that F-PEI/OVA/CpG could induce about 50% dendritic cells to become mature (Figure 7b). All these outcomes reveal a significant increase in DC cell maturation in cells treated with



F-PEI/OVA/CpG, which indicate that F-PEI/OVA/CpG could elicit robust antigen-presenting cell-mediated immune response.

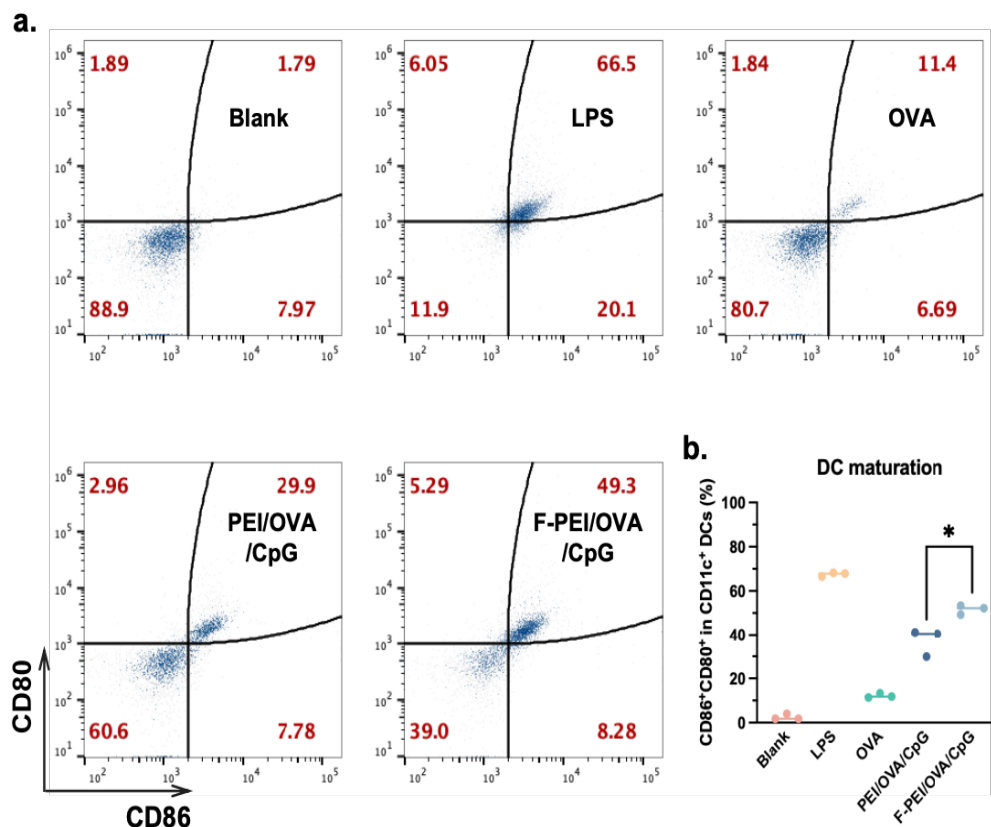


**Figure 7.** Efficiency of F-PEI/OVA nanovaccine to activate dendritic cells mature.

## Conclusions

This study provides a new strategy to design cancer vaccine, by the self-assembly of fluorinated PEI (F-PEI) into nanoparticles with negatively charged model antigens ovalbumin (OVA) and CpG ODN, the nanovaccine F-PEI/OVA/CpG was prepared. This approach could improve antigen delivery while simultaneously bolstering innate immunity by activating the TLR9 pathway, thus contributing to cellular immunity. First, the prepared F-PEI/OVA/CpG has a average diameter of 200 nm, and the DLS data displayed that the hydrodynamic size of F-PEI/OVA/CpG is  $256.7 \pm 2.1$ . Also, the CCK-8 results indicate that F-PEI/OVA/CpG posses good biocompatibility compared to PEI/OVA/CpG and the findings from FACS and fluorescence imaging collectively suggest the efficient cellular uptake of F-PEI/OVA/CpG. Further, the DC maturation assay revealed a significant increase in DC cell maturation in cells treated with F-PEI/OVA/CpG, which indicate that F-PEI/OVA/CpG could elicit robust antigen-presenting cell-mediated immune response. This project may yield a standardized method for preparing nanovaccines based on fluorinated polymers and provide insights into the extent to which vaccine efficiency can be enhanced through fluorination.

## Acknowledgments

In presenting this nanovaccine project, I want to acknowledge the support and guidance of my teacher, Mr. Wu, who has been critical in my experiment. His instruction has made my experiment successful and efficient. I also extend my thanks to Portsmouth abbey school and the Chinese academy for providing the resources I need. In addition, I want to appreciate all the scientists whose project I had referenced. Their efforts provide me with fundamental inspiration and memorable background knowledge for my project.

## Reference

- Zhang, Y. Y., Zhang, Z. M. (2020). The history and advances in cancer immunotherapy: understanding the characteristics of tumor-infiltrating immune cells and their therapeutic implications. *Cellular & Molecular Immunology*, 17 (8), 807-821. <https://doi.org/10.1038/s41423-020-0488-6>
- Wiemann, B.; Starnes, C. O. (1994). Coley's toxins, tumor necrosis factor and cancer research: a historical perspective. *Pharmacology & Therapeutics*, 64 (3), 529-564. [https://doi.org/10.1016/0163-7258\(94\)90023-x](https://doi.org/10.1016/0163-7258(94)90023-x)
- Rosenberg, S. A. (2011). Cell transfer immunotherapy for metastatic solid cancer--what clinicians need to know. *Nature Reviews Clinical Oncology*, 8 (10), 577-585. <https://doi.org/10.1038/nrclinonc.2011.116>
- Shiravand, Y., Khodadadi, F., Kashani, S. M. A., Hosseini-Fard, S. R., Hosseini, S., Sadeghirad, H., Ladwa, R., O'Byrne, K., Kulasinghe, A. (2022). Immune checkpoint inhibitors in cancer therapy. *Current Oncology*, 29 (5), 3044-3060. <https://doi.org/10.3390/curroncol29050247>
- Vermaelen, K. (2019). Vaccine strategies to improve anti-cancer cellular immune responses. *Frontiers in Immunology*, 10. <https://doi.org/10.3389/fimmu.2019.00008>. eCollection 2019
- Ribas, A., Wolchok, J. D. (2018). Cancer immunotherapy using checkpoint blockade. *Science*, 359 (6382), 1350-1355. <https://doi.org/10.1126/science.aar4060>
- Lehtinen, M., Dillner, J. (2013). Clinical trials of human papillomavirus vaccines and beyond. *Nature Reviews Clinical Oncology*, 10 (7), 400-410. <https://doi.org/10.1038/nrclinonc.2013.84>
- Shrestha, H., Bala, R., Arora, S. (2014). Lipid-based drug delivery systems. *Journal of pharmaceuticals*, 2014, 801820. <https://doi.org/10.1155/2014/801820>
- Bode, C., Zhao, G., Steinhagen, F., Kinjo, T., Klinman, D. M. (2011). CpG DNA as a vaccine adjuvant. *Expert Review of Vaccines*, 10 (4), 499-511. <https://doi.org/10.1586/erv.10.174>
- Krieg, A. M. (2006). Therapeutic potential of Toll-like receptor 9 activation. *Nature Reviews Drug Discovery*, 5 (6), 471-484. <https://doi.org/10.1038/nrd2059>
- Vivero-Escoto, J. L., Slowing, I. I., Trewyn, B. G., Lin, V. S. Y. (2010). Mesoporous Silica Nanoparticles for Intracellular Controlled Drug Delivery. *Small*, 6 (18), 1952-1967. <https://doi.org/10.1126/science.aar4060>

Neubi, G. M. N., Opoku-Damoah, Y., Gu, X. C., Han, Y., Zhou, J. P., Ding, Y. (2018). Bio-inspired drug delivery systems: an emerging platform for targeted cancer therapy. *Biomaterials Science*, 6(5), 958-973. <https://doi.org/10.1039/C8BM00175H>

Liechty, W. B., Kryscio, D. R., Slaughter, B. V., Peppas, N. A. (2010). Polymers for Drug Delivery Systems. *Annual Review of Chemical and Biomolecular Engineering*, 1, 149-173. <https://doi.org/10.1146/annurev-chembioeng-073009-100847>

Zhang, Z. J., Shen, W. W., Ling, J., Yan, Y., Hu, J. J., Cheng, Y. Y. (2018). The fluorination effect of fluoroamphiphiles in cytosolic protein delivery. *Nature Communications*, 9(1) 1377. <https://doi.org/10.1038/s41467-018-03779-8>

Cametti, M., Crousse, B., Metrangolo, P., Milani, R., Resnati, G. (2012). The fluororous effect in biomolecular applications. *Chemical Society Reviews*, 41 (1), 31-42. <https://doi.org/10.1039/c1cs15084g>